

# Kerr Nonlinear Characteristics of Plasmonic Waveguide Devices

Guangyuan Li<sup>1,2,\*</sup>, C. Martijn de Sterke<sup>1,2</sup>, and Stefano Palomba<sup>1,\*</sup>

<sup>1</sup>Institute of Photonics and Optical Science (IPOS), School of Physics, The University of Sydney, NSW 2006, Australia

<sup>2</sup>Centre for Ultrahigh bandwidth Devices for Optical Systems (CUDOS), School of Physics, The University of Sydney, NSW 2006, Australia

Email: guangyuan.li@sydney.edu.au; stefano.palomba@sydney.edu.au

**Abstract**—Plasmonic waveguides are promising in nonlinear optical applications because of their subwavelength field confinement, which can strongly enhance light-matter interactions and greatly reduce the device footprint. We investigate the Kerr nonlinear characteristics of two typical plasmonic waveguides and compare their relative merits to a conventional all-dielectric silicon slot waveguide. This work provides useful guidance on designing ultra-compact nonlinear optical devices.

## I. INTRODUCTION

Compact integrated nonlinear photonic chips, operation at low power level and high efficiency, has been attracting much attention in applications such as all-optical generation and signal processing [1]–[3]. For Kerr-type nonlinearity, strong nonlinear effects or equivalently large nonlinear coefficient  $\gamma$  can be achieved by using either strong nonlinear materials or small effective mode area [4]. By confining the electromagnetic fields beyond the diffraction limit and thus greatly enhancing light-matter interactions, plasmonic waveguides have been predicted to be a promising platform for efficient Kerr nonlinear devices on the scale of micrometers [5] even though they exhibit absorption. Calculations have shown that the nonlinear coefficient of a plasmonic waveguide reaches  $\gamma \sim 10^7 \text{ W}^{-1} \text{ km}^{-1}$  [6], [7], orders of magnitude larger than conventional all-dielectric waveguides. Four wave mixing (FWM) was also experimentally observed in a  $10 \mu\text{m}$  hybrid-plasmonic waveguide by Diaz et al [8]. However, the effect was weak and more work is required to design and optimize such structures for better nonlinear device performance.

Recently we the generalized full-vectorial nonlinear Schrödinger equation governing nonlinear pulse propagation in a lossy waveguide, derived the power threshold allowed in such a highly confined waveguide by taking into account the local field enhancement and the material damage threshold, and proposed a simple and versatile FOM for Kerr nonlinear waveguides with linear losses [9]. Based on these results, here we investigate the Kerr nonlinear characteristics of two typical plasmonic waveguides and compare their merits with a conventional all-dielectric waveguide.

## II. RESULTS AND DISCUSSION

We consider two typical plasmonic waveguide configurations, namely an all-plasmonic waveguide (noted as APW) and

a hybrid-plasmonic waveguide (HPW), and compare them with an all-dielectric silicon-slot waveguide (ADW) (see Fig. 1(a)). All of these incorporate a slot filled with DDMEBT, a highly nonlinear polymer [10]. To ensure a fair comparison, the same structure and identical material parameters are used except that the ridges are silver-slot-silver (from top to bottom) for the APW, and silver-slot-silicon for the HPW, and silicon-slot-silicon for the ADW. All the waveguide eigenmodes were analyzed numerically using COMSOL with  $w = h = 220 \text{ nm}$ ,  $\lambda = 1550 \text{ nm}$ ,  $n_{\text{SiO}_2} = 1.45$ ,  $n_{\text{Ag}} = 0.144 + 11.366i$  [11],  $n = 3.477$  and  $n_2 = 2.5 \times 10^{-18} \text{ m}^2 \text{ W}^{-1}$  for silicon [12],  $n = 1.8$  and  $n_2 = 1.7 \times 10^{-17} \text{ m}^2 \text{ W}^{-1}$  for DDMEBT [10]. We estimate the DDMEBT damage threshold to be  $I_{\text{th}} = 5 \text{ GW cm}^{-2}$ , which is inferred from experiments [10]. The slot thickness  $h_s$  was varied between 5 nm and 200 nm in steps of 10 nm. The attenuation losses of the APW and the HPW are assumed to be absorption losses, and that of the ADW to be scattering loss, which is taken to be independent from  $h_s$  for simplicity, and the corresponding attenuation length is taken to be  $L_{\text{ATT}} = 1.89 \text{ mm}$  [13].

We characterize a lossy nonlinear waveguide as follows. The effective mode area  $A_{\text{eff}}$  defined in [14] is used as a measurement of the mode confinement. The nonlinear coefficient  $\gamma$  defined in [14] determines the magnitude of the nonlinear effects. The power threshold  $P_{0,\text{th}}$  defined in [9] means the maximum pump power allowed in the waveguide. The nonlinear length  $L_{\text{NL}} \equiv 1/(\gamma P_0)$  [4] provides the length scale over which the nonlinear effects become important. Our previously proposed and validated figure of merit,  $\mathcal{F} \equiv \gamma L_{\text{ATT}} P_{0,\text{th}}$ , determines the maximum achievable degenerate four wave mixing conversion efficiency as,  $\eta_{\text{max}} = 4\mathcal{F}^2/27$ , and the nonlinear phase shift as  $\Delta\Phi_{\text{NL}} = 2\mathcal{F}/3$ , at the optimal waveguide length  $L_{\text{OPT}} = \ln 3 \cdot L_{\text{ATT}} \approx 1.1L_{\text{ATT}}$  [9].

Using these measures, the APW, the HPW and the ADW are compared in Figs. 1(b)–1(f). Figure 1(b) shows that the effective mode area of the APW can be as small as  $0.002(\lambda/2)^2$ , far below the diffraction limit, while that of the HPW can reach  $0.04(\lambda/2)^2$ , and that of the ADW is always larger than  $0.1(\lambda/2)^2$ . Accordingly, the nonlinear coefficients reach values as high as  $\gamma = 8.3 \times 10^8 \text{ W}^{-1} \text{ km}^{-1}$  for the APW and  $\gamma = 5.7 \times 10^6 \text{ W}^{-1} \text{ km}^{-1}$  for the HPW, and only  $\gamma = 1.4 \times 10^6 \text{ W}^{-1} \text{ km}^{-1}$  for the ADW, as shown in

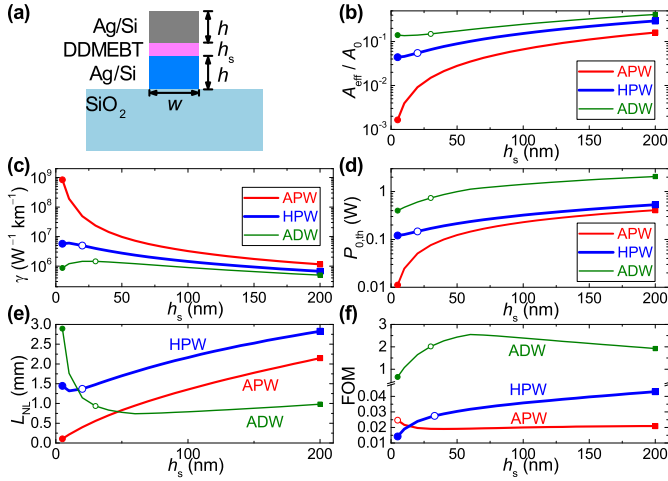


Fig. 1. (a) Schematics of the APW, HPW, and ADW structures. (b)  $A_{\text{eff}}/A_0$  with  $A_0 = (\lambda/2)^2$ , (c)  $\gamma$ , (d)  $P_{0,\text{th}}$ , (e)  $L_{0,\text{NL}}$ , (f)  $\mathcal{F}$  versus  $h_s$ . The waveguides selected for further study are indicated by open circles.

Figs. 1(c). Thus, in terms of mode confinement and nonlinear coefficient, the APW is better than the HPW and much better than the ADW. However, tighter confinement leads to stronger electric field enhancement, and thus lowers the maximum power allowed in the waveguide,  $P_{0,\text{th}}$ , as shown in Fig. 1(d). Combining Figs. 1(c) and 1(d), the nonlinear length is shown in Fig. 1(e). Results show that  $L_{\text{NL}}$  can be as short as  $100\ \mu\text{m}$  for the APW, compared with  $740\ \mu\text{m}$  for the ADW. Figure 1(f) shows that  $\mathcal{F}$  of the APW and HPW are two orders of magnitude smaller than that of the ADW. As a result, if a nonlinear phase shift of order  $\pi$  is required, or a high conversion efficiency, the ADW is the best candidate. In contrast, if low-power operation or small device footprint is crucial, the APW is preferred.

To illustrate the nonlinear performance of the three particular waveguide configurations, an APW with  $h_s = 5\ \text{nm}$ , an HPW with  $h_s = 20\ \text{nm}$  and an ADW with  $h_s = 30\ \text{nm}$ . We optimize each of them separately for four-wave mixing efficiency  $\eta$ , making sure that their power thresholds are not exceeded, using an approximate analytic solution that we validated previously [9]. As an example, for an input power of  $P_0 = 10\ \text{mW}$ , Fig. 2 confirms that the APW has the highest conversion for short waveguide lengths ( $L < 19\ \mu\text{m}$ ), the HPW is more favorable for intermediate lengths ( $19 < L < 43\ \mu\text{m}$ ), while the ADW is best if a large footprint is not an issue.

### III. CONCLUSION

In conclusion, we compare the Kerr nonlinear properties two typical plasmonic waveguide configurations, the all-plasmonic waveguide and the hybrid-plasmonic waveguide, and compare with a low-loss all-dielectric silicon slot waveguide. We find that the all-plasmonic waveguide is the best choice for low-power operation and ultra-compact integration, followed by the hybrid-plasmonic waveguide, but both plasmonic waveguides suffer from limited nonlinear phase shift and conversion efficiency due to losses. The all-dielectric waveguide is best

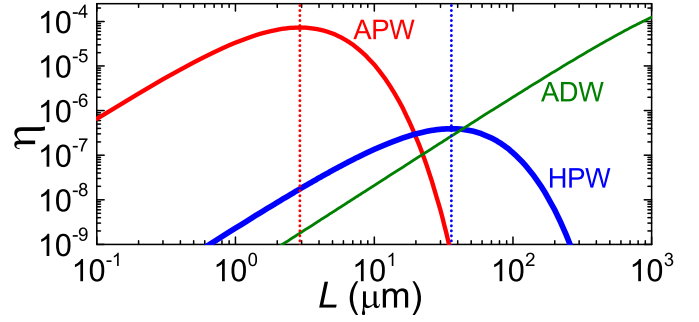


Fig. 2. Comparison of the conversion efficiency  $\eta$  of the APW, the HPW and the ADW versus the waveguide length  $L$ , for  $P_0 = 10\ \text{mW}$ . Vertical lines indicate the optimal waveguide lengths  $L_{\text{OPT}}$ .

if a large nonlinear phase shift or high conversion efficiency are required in applications such as optical switching. These results provide theoretical guidance in choosing the most suitable waveguide geometry.

### ACKNOWLEDGMENT

This work was funded by the Australian Research Council (Discovery Projects scheme, DP150100779).

### REFERENCES

- [1] J. Leuthold *et al.*, “Silicon organic hybrid technology a platform for practical nonlinear optics,” *Proc. IEEE*, vol. 97, pp. 1304–1316, 2009.
- [2] D. J. Moss, R. Morandotti, A. L. Gaeta, and M. Lipson, “New CMOS-compatible platforms based on silicon nitride and hybrid for nonlinear optics,” *Nature Photon.*, vol. 7, pp. 597–607, 2013.
- [3] S. Wabnitz and B. J. Eggleton, *All-Optical Signal Processing: Data Communication and Storage Applications*. New York: Springer, 2015.
- [4] G. P. Agrawal, *Nonlinear Fiber Optics*, 5th ed. New York: Elsevier, 2013.
- [5] J. R. Salgueiro and Y. S. Kivshar, “Nonlinear couplers with tapered plasmonic waveguides,” *Opt. Express*, vol. 20, pp. 9403–9408, 2012.
- [6] M. M. Hossain, M. D. Turner, and M. Gu, “Ultra-high nonlinear nanoshell plasmonic waveguide with total energy confinement,” *Opt. Express*, vol. 19, pp. 23 800–23 808, 2011.
- [7] A. Pitolakis and E. E. Kriezis, “Highly nonlinear hybrid silicon-plasmonic waveguides: analysis and optimization,” *J. Opt. Soc. Am. B*, vol. 30, pp. 1954–1965, 2013.
- [8] F. J. Diaz *et al.*, “Sensitive method for measuring third order nonlinearities in short dielectric and hybrid plasmonic waveguides,” *Opt. Express*, vol. 24, pp. 545–554, 2016.
- [9] G. Li, C. M. de Sterke, and S. Palomba, “Figure of merit for Kerr nonlinear plasmonic waveguides,” (*in review*).
- [10] B. Esemeson, M. L. Scimeca, T. Michinobu, F. Diederich, and I. Biaggio, “A high-optical quality supramolecular assembly for third-order integrated nonlinear optics,” *Adv. Mater.*, vol. 20, pp. 4584–4587, 2008.
- [11] P. B. Johnson and R. W. Christy, “Optical constants of the noble metals,” *Phys. Rev. B*, vol. 6, pp. 4370–4379, 1972.
- [12] Q. Lin *et al.*, “Dispersion of silicon nonlinearities in the near infrared region,” *Appl. Phys. Lett.*, vol. 91, p. 021111, 2007.
- [13] C. Koos *et al.*, “Highly-nonlinear silicon photonics slot waveguide,” *OFC/NFOEC*, p. PDP25, 2008.
- [14] V. S. Afshar, T. M. Monro, and C. M. de Sterke, “Understanding the contribution of mode area and slow light to the effective Kerr nonlinearity of waveguides,” *Opt. Express*, vol. 21, pp. 18 558–18 571, 2013.